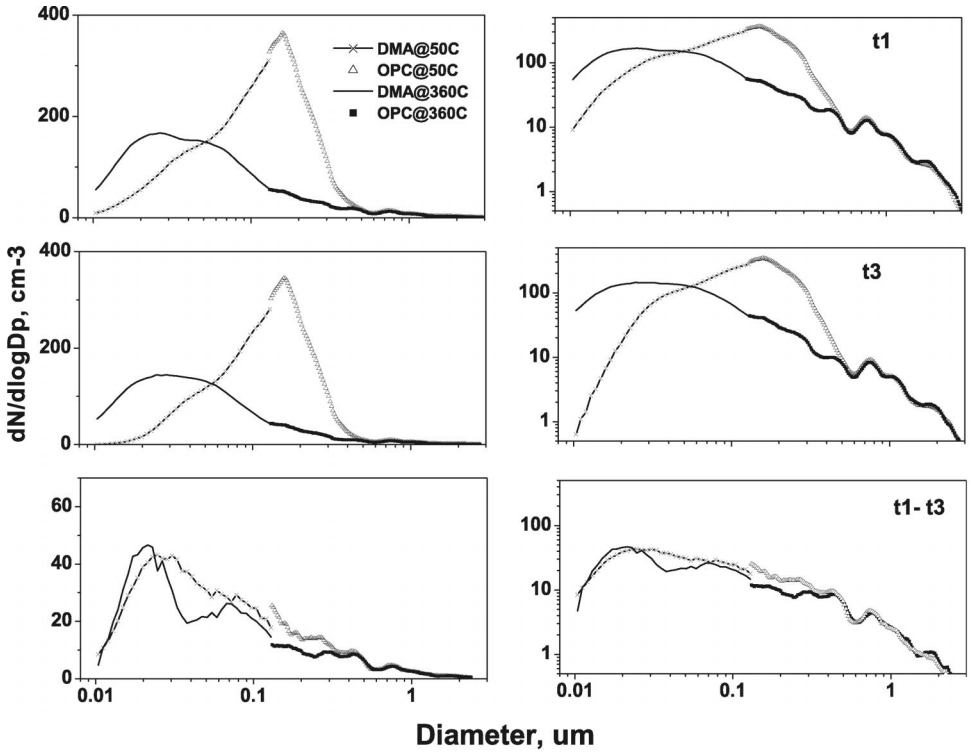

FIG. 4. Dry number size distributions (DOY 119) measured at (top) 5 and (middle) 20 m and (bottom) their difference for unheated (50°C) and heated refractory distributions (360°C) in both linear and logarithmic concentration formats (10-point-diameter smoothing applied).

2003), refractory species other than sea salt are possible. Such thermally resolved sea-salt sizes (Clarke et al. 1993; O'Dowd et al. 1997) also provide a tool for interpreting other measurements of sea salt (Campuzano-Jost et al. 2003).

The contribution of coastal breaking waves is clearly revealed by the difference between number distributions at 20 and 5 m (Fig. 4, lower panels). The unheated difference distribution demonstrates that breaking waves produce particles from as small as 0.01 μm (dry diameter) up to several micrometers (larger sizes not shown here) and with a number peak near 0.03–0.40 μm. The heated difference distributions show that most of these are refractory at 360°C, consistent with their being sea salt. The average heated and unheated difference distributions are similar in both their number and shape, indicating that these small particles produced are refractory. The lower number at the smallest sizes for the RDMA measurements is presumably due to the 360°C RDMA scan always being the last sample from the LAG chamber, leading to diffusive losses for smaller particles that have not been corrected for here. Even so, the integral number of about 30–40 cm^{-3} is consistent with the typical number peaks evident in the CNcold and CNhot from breaking waves at the 5-m level (Fig. 3). The shapes of these difference distributions are also similar to the total refractory distributions measured at both altitudes. This suggests that sea salt from breaking waves in open-ocean conditions probably contributes to these refractory aerosols. These sizes are far smaller than the 0.1–0.2-μm diameters often referenced in the literature for the smallest sizes of sea-salt size distributions (Hoppel et al. 2002, and references therein).

Coarse particles from breaking waves were also characterized through similar differencing of data collected at the top and bottom of the tower. However, because concentrations are much lower for coarse aerosol, we use averages of each 20-min sample from each altitude accumulated over many hourly cycles. These coarse-particle distributions also require some corrections for inlet losses of coarse particles, as discussed below. Resulting difference distributions for the bottom less the top of the tower are shown in Fig. 5a as number distributions on a logarithmic scale. The sea-salt mass and the sizes that dominate observed scattering are best revealed in Fig. 5b as linear volume distributions (multiply the scale by about 2 to estimate area under curve as dry mass in $\mu g\ m^{-3}$). These difference distributions show that these coastal breaking waves produce aerosol dry mass that peaked near 7 μm. If growth to typical ambient humidity (RH 80%) is estimated for the dry sizes shown here, they would nearly double in size. The resulting concentration and the falloff in coarse-particle number concentration with size would be very similar to the recently published ambient data of Hoppel et al. (2002) for 10 m s^{-1} near-surface winds.

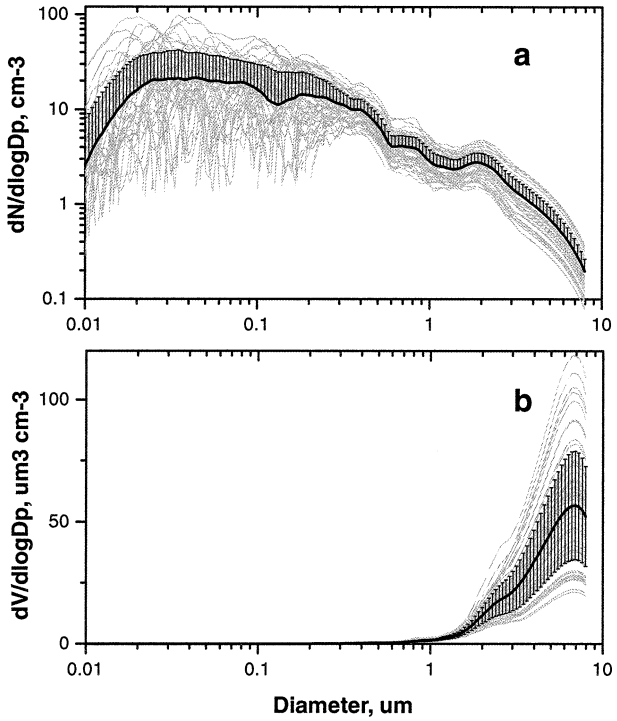

FIG. 5. A superposition of dry (a) number and (b) volume size distributions obtained by differencing the average 5- and 20-m tower data obtained for each hourly cycle during SEAS. The transmission correction to the UH inlet has been applied. Single leg std dev shown on log plot for clarity.

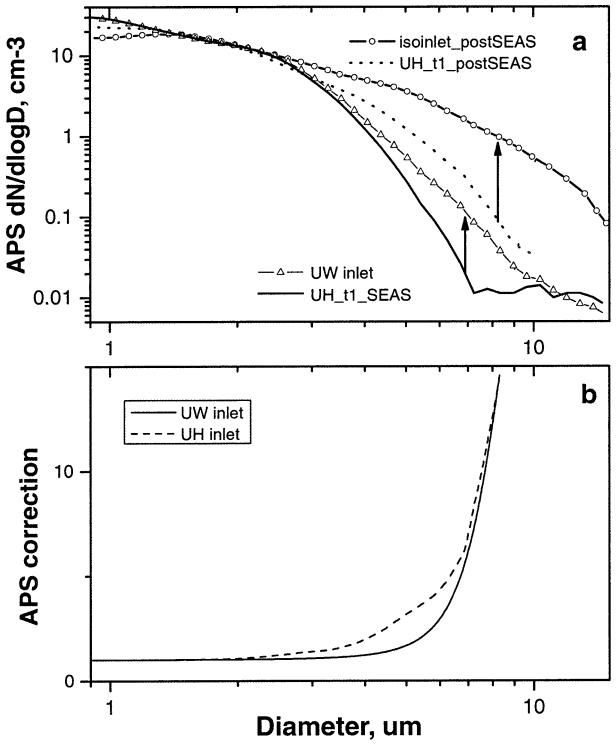

FIG. 6. (a) Comparison of measured APS size data for UH tower inlet t1 (solid line) vs UW inlet (triangles) during SEAS using an old APS with a ''ghost'' particle counting problem, and a similar post-SEAS comparison for a new APS (no inlet) vs UH tower inlet t1 measured with new APS. Arrows indicate curves to be compared in each case (see text). (b) APS inlet correction factor based upon data in (a).

c. Inlets, size distributions, and calibration issues

The UH and UW inlets were different, and an assessment of inlet performance as a function of aerosol size is needed if quantitative comparison to ambient conditions is attempted for the UW nephelometer. The inlet to the UW nephelometer did not have the valves present in the UH system. Also the UH system employed a PVC tube located at about 10 m on the tower compared to about 11 m for the UW nephelometer (Masonis et al. 2003) that also operated at a higher RH. In order to test for sampling differences in the UH and UW inlets under similar conditions the APS was removed from the UH inlet and operated on the UW inlet upstream of the UW nephelometer and then returned to the UH inlet. Comparison of APS size data (Fig. 6a) at 55% RH for the UH and UW inlets during SEAS shows that both inlets had similar transmission (Fig. 6b) for particles sizes up to about 2 μm. Above that size, the UH system was less efficient up to about 7 μm. Figure 6b shows the different size-dependent corrections used for UH and UW inlets based upon the ratio between the UH (t3) and UW inlets. Above 7 μm, the UH inlet sizes show a sudden inflection and evidence of irregular counting that is nearly constant with size. Similar behavior is also evident above 10 μm for the same APS on the UW inlet. We now believe that this behavior is linked to ''ghost'' particles circulating inside the APS sensing volume that yield pulses interpreted as additional larger aerosol at random sizes (M. Havlicek, TSI, 2000, personal communication). These are most conspicuous when the actual large-particle concentrations are low, and they result in a combination of real and artifact counts at larger sizes that are difficult to separate.

The new TSI APS Model 3321 corrects this ''ghost'' problem and was deployed after SEAS on 2 April 2002, under similar conditions at the BAFS tower and operated with a short 10-cm isokinetic inlet directly into the wind (about 3 m s^{-1}) at 5 m (tl). Figure 6a shows size distributions collected over 30 min from this inlet (isoinlet_post SEAS) and those after sequential sampling for 30 min through the SEAS 5-m inlet (UH_t1_post SEAS). These distributions are normalized to sizes at 1.5 μm, where inlet losses are not evident, in order to compare to data from different periods. This comparison confirms both the unrealistic shape of the distributions for the SEAS data above about 7 μm as well as the significant coarse-particle losses through the SEAS inlet. Hence the SEAS tower size data suffered from loss of coarse particles in the inlet that reduced coarse concentrations to where ghost particles artificially enhanced coarse concentrations over those present at the APS. Figure 6a reveals that a direct correction of APS data above 7 μm